

# Paleoceanography and Paleoclimatology®

## RESEARCH ARTICLE

10.1029/2024PA004974

### Key Points:

- A pronounced isotopic enrichment trend is observed from 3.9 to 3.6 ka in a network of Asian speleothem records
- This trend is observed in records influenced by both the Indian Summer Monsoon and the East Asian Summer Monsoon
- This network fails to show a spatially coherent isotopic signal around the 4.2 ka event interval

### Supporting Information:

Supporting Information may be found in the online version of this article.

### Correspondence to:

A. James,  
[akjames@usc.edu](mailto:akjames@usc.edu)








### Citation:

James, A., Hu, J., Emile-Geay, J., Partin, J. W., Scroton, N., Malik, N., & Gao, Y. (2025). Regime shifts in Holocene paleohydrology as recorded by Asian speleothems. *Paleoceanography and Paleoclimatology*, 40, e2024PA004974. <https://doi.org/10.1029/2024PA004974>

Received 11 JUL 2024

Accepted 10 DEC 2024

## Regime Shifts in Holocene Paleohydrology as Recorded by Asian Speleothems

Alexander James<sup>1</sup> , Jun Hu<sup>2</sup> , Julien Emile-Geay<sup>1</sup> , Judson W. Partin<sup>3</sup> , Nick Scroton<sup>4</sup> , Nishant Malik<sup>5</sup> , and Yuan Gao<sup>2</sup> 

<sup>1</sup>Department of Earth Sciences, University of Southern California, Los Angeles, CA, USA, <sup>2</sup>College of Ocean and Earth Sciences, Xiamen University, Xiamen, China, <sup>3</sup>Institute for Geophysics, Jackson School of Geosciences, University of Texas at Austin, Austin, TX, USA, <sup>4</sup>Department of Geography, Irish Climate Analysis and Research Units (ICARUS), Maynooth University, Maynooth, Co. Kildare, Ireland, <sup>5</sup>School of Mathematics and Statistics, Rochester Institute of Technology, Rochester, NY, USA

**Abstract** Speleothem oxygen isotope records offer unique insights into Asian Monsoon evolution, with their precise chronologies used to identify abrupt climatic events. However, individual records are sometimes used to draw broad conclusions about global climate, without considering the dynamical context in which they exist. We present a robust framework for assessing the regional significance, and hence the potential global significance, of paleoclimate events, using the proposed Meghalayan age onset (associated with the “4.2 ka event”) as a case study. Analyzing 14 well-dated speleothem oxygen isotope records from the SISAL v3 database and recent literature, we investigate the regional coherency of rapid shifts in Asian paleohydrology, which is the regional center of action for the proposed event, over the Holocene. Three robust methods fail to detect spatially coherent variability consistent with a 4.2 ka event across Asia, either because none exists or because it is of insufficient magnitude. In contrast, the 8.2 ka event is expressed in most records that resolve it. The absence of a clear isotopic excursion across this data set suggests that the “4.2 ka megadrought” was not global, with important implications for archeology and geochronology. This casts doubt on the proposal that the 4.2 ka event marks the onset of a new geologic age. We do, however, observe support for a gradual isotopic enrichment between 3.9 and 3.6 ka, followed by partial recovery—consistent with the “Double Drying” hypothesis and possibly related to changes in El Niño–Southern Oscillation variability.

**Plain Language Summary** Cave formations, known as speleothems, preserve valuable records of past climate. We analyzed 14 of these records to examine a proposed global drought that occurred about 4,200 years ago, centered in South Asia. This event, called the “4.2 ka event,” is thought to have contributed to the fall of several ancient civilizations and currently marks the beginning of our most recent geologic age. However, our study found little evidence of a widespread drought across Asia during this time. We developed a robust framework to assess the regional/global importance of past climate events, addressing concerns about using limited data to draw broad conclusions. While we didn't find strong support for the 4.2 ka event, we observed clear signs of an earlier, globally significant climate shift around 8,200 years ago. Interestingly, we discovered a consistent pattern of gradual drying over thousands of years, with a more pronounced dry period between 3,900 and 3,600 years ago. This drying, possibly linked to changes in Pacific Ocean surface temperature patterns, affected areas influenced by both the Indian and East Asian monsoons. Our findings challenge the global significance of the 4.2 ka event and highlight the importance of querying multiple records when studying past climate changes.

## 1. Introduction

Speleothem records are now a mainstay of paleohydrology, often displaying high temporal precision thanks to U-Th dating techniques (Cheng et al., 2013; Shen et al., 2012, 2013), and supporting many high-resolution data streams (McDermott, 2004). Most of these records come in the form of stalagmites, which are columnar speleothems that form on cave floors. While oxygen isotope records ( $\delta^{18}\text{O}$ ) from speleothems have varied interpretations depending on the geochemical controls on source water, surface hydrology, and calcification processes (Lachniet, 2009), Asian speleothem  $\delta^{18}\text{O}$  series have been widely interpreted as records of Asian monsoon intensity over orbital scales (Cheng et al., 2016; Y. Wang et al., 2001). Exemplar speleothem  $\delta^{18}\text{O}$  records can cover several of Earth's orbital cycles (which range from ~20 to 400 thousand years (Adhémar, 1842))

and display coherent variability in phase with local insolation, particularly at precessional periods, circa 19 and 23 kyrs (Battisti et al., 2014; Cheng et al., 2016; P. Wang et al., 2005; Y. Wang et al., 2008). While the monsoon interpretation is robust—though complex (J. Hu et al., 2019)—at orbital scales, it may not hold at shorter timescales of centuries to millennia (Y. Li et al., 2014; Wan et al., 2011).

This is of critical importance, as speleothem records are increasingly used in archeology (Westaway et al., 2007), geology (Bard et al., 2002), and geochronology (Berkelhammer et al., 2013), with the latter the subject of a recent controversy (Voosen, 2018). In 2018, the International Commission on Stratigraphy (ICS) formally ratified a proposal to subdivide the Holocene Epoch (Walker et al., 2018) into three shorter segments, the most recent of which (the Meghalayan age) is named after a stalagmite record (KM-A) from Mawmluh cave (Berkelhammer et al., 2013) in the Indian state of Meghalaya. This definition is based on an abrupt shift in  $\delta^{18}\text{O}$  observed circa 4.2 ka before present (BP) in that record, and interpreted as representative of the Indian monsoon as a whole (Berkelhammer et al., 2013). This isotopic excursion now serves as the Global Stratotype Section and Point (GSSP) of the Meghalayan age (4200 yr BP to present), which, as the name implies, signals a change of global significance. Should its interpretation change, or should a 4.2 ka anomaly fail to be widely expressed in speleothem records from the region, it would have important implications for this chronological delineation—and for the wider use of speleothem records on sub-orbital timescales.

Indeed, there exist several abrupt hydroclimate excursions between 4.2 and 3.9 ka, documented in diverse proxy archives across the Middle East (Arz et al., 2006; Cullen et al., 2000; Stanley et al., 2003), the Mediterranean (Drysdale et al., 2006; Psomiadis et al., 2018), South and East Asia (Berkelhammer et al., 2013; Liu & Feng, 2012; Staubwasser et al., 2003), East Africa (Thompson et al., 2002), and North America (Fisher et al., 2008; Menounos et al., 2008). This string of events in paleoclimate records has led the “4.2 ka event” to be characterized as a global megadrought (Weiss, 2016). In addition to geochemical evidence, archeological work shows that this time period coincides with the collapse of several civilizations across Eurasia and North Africa, including the Akkadian Empire in Mesopotamia (which collapsed ca 4170  $\pm$  150 BP) (Cullen et al., 2000; Weiss et al., 1993), the Old Kingdom of Egypt (whose disintegration started around 4200 BP) (Butzer, 2012; Stanley et al., 2003), the Harappan civilization in the Indus Valley (declining by 3900 BP) (Staubwasser et al., 2003), and the Longshan culture and other Neolithic cultures in China (which collapsed around 4200–3900 BP) (G. Jin & Liu, 2002; Liu & Feng, 2012; Wu & Liu, 2004; H. Zhang, Cheng, et al., 2021).

However, a wider examination of additional proxy records appears to contradict the notion of a global megadrought circa 4.2 ka, as many proxy records, such as speleothem oxygen isotopes, peatland multi-proxy reconstructions, marine isotopic records, and others, show wet or unremarkable hydroclimate anomalies at that time (Constantin et al., 2007; H. Li et al., 2018; Railsback et al., 2018; Roland et al., 2014; Scroxton et al., 2023b). Furthermore, where a dry event is present, its timing remains uncertain in many records (Kathayat et al., 2018; Railsback et al., 2018; Staubwasser & Weiss, 2006).

Many of these studies were focused on presenting and interpreting new data from a given field campaign. However, due to the noisy nature of paleoclimate data, data synthesis offers advantages over individuated analysis when constraining the spatial extent of a proposed climate phenomenon (Jonkers et al., 2021). There are two main poles that define the spectrum of data synthesis study structure. The first approach prioritizes high data volumes, collating as much data as possible before carrying out quantitative analysis. This structure produces very robust results, but makes detailed high-resolution analysis difficult. The second is a high-resolution, low-volume approach. Such studies perform more detailed analysis on a smaller subset of hand-picked records, sacrificing a degree of robustness for the ability to draw more detailed conclusions.

Within the context of the 4.2 ka event, both the high-volume (McKay et al., 2024; Parker & Harrison, 2022) and the high-resolution (Scroxton et al., 2023b) approaches to data synthesis have suggested that the 4.2 ka event was not globally significant. However, Scroxton et al. (2023b) presented evidence for a “Double Drying Hypothesis,” which suggests that there are three patterns of drying present in regions governed by the Indian monsoon during the mid-Holocene. Pattern 1 is a secular drying trend that is present for the duration of the Holocene, and is associated with changing insolation. Pattern 2 is a brief period of enhanced drying from roughly 3.9 to 3.5 ka that appears in records from around the Indian Ocean basin. Pattern 3 expresses a 4.2 ka event, that is, a period of extreme aridity that appears in select paleo-proxies from the same region during the interval from roughly 4.2 to 4 ka. Type examples of each of these patterns can be found in Figure 2 of Scroxton et al. (2023b).

To further ascertain the spatio-temporal footprint of the 4.2 ka event, this work assesses its expression in Asia using the most up-to-date data sets and three independent detection methods. We assemble a network of 14 high-resolution, precisely-dated speleothem oxygen isotope records from Asia, on which we systematically apply a suite of robust statistical analyses including interval statistics, Laplacian Eigenmaps for Recurrence Matrices (LERM), and Monte-Carlo Principal Component Analysis (MC-PCA), each of which take age uncertainty explicitly into account. Our results reveal no evidence for a widespread 4.2 ka event in Asian speleothems, challenging the notion of a global megadrought. Instead, we find strong support for two of the three patterns proposed by the Double Drying hypothesis: a gradual enrichment of  $\delta^{18}\text{O}$  values over the Holocene, and a more pronounced enrichment episode from 3.9 to 3.5 ka. We do not propose that the 4.2 ka event occurred during 3.9–3.5 ka rather than its canonical 4.2–4 ka interval. Instead, we find evidence that there was a separate period of enrichment during the 3.9–3.5 ka interval. Given the growing literature on drying at 3.9 kyr BP (Giesche et al., 2018; Giosan et al., 2018; Leipe et al., 2014; Scroton et al., 2023b), and the increased temporal and dating resolution of paleoclimate records, it is now highly likely that these are two different climate excursions with different drivers. We note that these kinds of enrichment episodes are often interpreted as reflecting regional drying (Fairchild & McMillan, 2007) (the “amount effect”). While this interpretation is well supported over oceanic islands like Borneo (Moerman et al., 2013), it may break down over large continental masses like Asia, where other competing effects may prevail (J. Hu et al., 2019). In the following, we thus refrain from translating  $\delta^{18}\text{O}$  values to local precipitation. However, in certain cases (e.g., when placing our findings within the context of Scroton et al. (2023b)), we borrow the amount effect interpretation and use “drying” as a shorthand for isotopic enrichment.

The remainder of this paper is structured as follows. In Section 2, we describe the data sets and methodologies employed in our analysis. Section 3 presents the key findings that emerge from this analysis. Then, Section 4 discusses these results in a broader paleoclimatic context, and reflects on their implications for our understanding of the 4.2 ka event and Holocene hydroclimate variability more generally.

## 2. Data and Methods

### 2.1. Evidentiary Standard

While many articles have discussed paleoclimate events, few have explicitly stated their criteria for defining such events. At a minimum, we claim that a spatially coherent paleoclimate event should stand out as a clear, well-dated excursion in a geographically wide network of paleoclimate proxies of appropriate resolution. If the event is claimed to be globally significant, it should appear in a large majority of records. If the event is regionally significant, it should also stand out in a collection of suitable records, though covering a smaller area of the globe. For instance, if an event is claimed to be representative of the Indian Summer Monsoon (ISM), it should be detectable in most areas presently affected by the ISM. Global significance implies regional significance: if an event is not regionally significant, it cannot be globally significant. However, some allowance should be made for non detection as proxy sensitivity and seasonal biases may obscure otherwise impactful climate signals.

A distinction should be made here between global significance and global impact. Most climate events are likely to have a well-defined signal around some geographic center of origin, with the amplitude of the signal decaying with distance from that center. Additionally, there will be some teleconnections that propagate the signal with minimal loss of amplitude. This means that an event which stands out in one region may be comparable to centennial-scale variability in another, and an undetectable part of noise in others. Identification of a climate event in a particular area is important to characterize the spatial extent of that climate event, regardless of whether it is significantly different from centennial-scale variability. For instance, while both the 8.2 and 4.2 ka events are present in speleothems from Madagascar, they do not stand out against the backdrop of natural variability (Dawson et al., 2024; Scroton et al., 2023a; Williams et al., 2023). That is, while they had an “impact,” they are not “significant.” This suggests that, while these events did not have a strong influence on the climate in Madagascar, the climate system is set up in such a way as to propagate their influence to the region. In this study, we are primarily concerned with evaluating the global significance, rather than the global impact, of the 4.2 ka event. To do so, we explore the regional impact of the event near its proposed epicenter. We focus on regional impact as we expect an event that is globally significant to, at minimum, be regionally impactful. If we do not observe an impactful event within the region that contains the event’s proposed epicenter, then claims of global significance should be viewed with skepticism.

**Table 1**  
*Asian Speleothem Records Used in This Study*

Cave site	Stalagmite name	Lat.	Lon.	Time range (y BP)	Chron control (y)	Resolution (y)	Reference
Heshang	HS4	30.45	110.42	9458, 82	59, 158	3	C. Hu et al. (2008)
Jiuxian	C996-1	33.57	109.1	7841, −4	230, 1880	5	Cai et al. (2010)
Lianhua	LH-2	29.48	109.53	12431, 51	17,219	10	H.-L. Zhang et al. (2013)
Mawmluh	KM-A	25.26	91.82	12107, 3654	32, 480	6	Berkelhammer et al. (2013)
Xianglong	XL26	33.00	106.33	6657, 2008	20, 31	9	Tan et al. (2018)
Dongge	DA	25.28	108.08	8902, −20	63, 128	4	Y. Wang et al. (2005)
Sahiya	SAH-2	30.6	77.87	5648, 2607	79.5, 155	1	Kathayat et al. (2017)
Hoq	Hq-1	12.59	54.35	9249, −46	30, 90	14	Van Rangelbergh et al. (2013)
Jiulong	JL1	27.8	113.9	7271, 102	224, 1030	12	H. Zhang, Cheng, et al. (2021)
Liuli	LL2	41.02	125.82	6683, −55	123, 523	10	Zhao et al. (2021)
Guizhouxinv	GZXND21-1	27.1	105.1	5866, 3665	18, 28	1	Y. Li et al. (2023)
Tangga	TA12-2	−0.36	100.76	16571, 159	97, 304	14	Wurtzel et al. (2018)
La Vierge	LAVI-4	−19.8	63.4	6014, 2999	79, 198	3	H. Li et al. (2018)
Oman	Q5	17.17	54.3	10874, 402	28, 132	5	Tian et al. (2023)

*Note.* “Chron control” describes the median and maximum  $2\sigma$  uncertainties associated with the radiometric tie points used to generate the record's age ensemble. Resolution refers to the median spacing between consecutive observations between 10,000 and 0 Years BP. BP means “before 1950 AD.” All time units here are given in years.

The first step in testing both the spatial impact and/or significance of an event must then be to assemble a network of qualified proxy records into a testing data set. To address our motivating question, we require records that meet the following criteria:

**Sufficient length:** Each record should provide appropriate context for the event. The event should not lie at the edge of the record, and the record should be long enough to contextualize the event within the broader climate history of the region. Here we use a padding requirement of 700 years, roughly three times the length of the event, and a minimum length requirement of 3000 years in total. Allowances were made here for the record from Guizhouxinv, as it has high resolution and nearly meets these requirements, and Mawmluh, as it is the canonical example of the 4.2 ka event.

**Sufficient resolution:** The choice of appropriate minimum resolution is a subjective one. Here we use a minimum resolution of 15 years, roughly 10 percent of the purported length of the event. This resolution gives us a good chance of detecting the event without restricting record availability too severely.

**Chronological control:** Records should have age uncertainties around the event that are substantially smaller than the event's proposed duration. These uncertainties can be estimated from the reported standard deviations of the chronological constraints (e.g., U-Th dates) near the event. For this study, we preferentially selected records with at least two age control points within 100 years of the 4.2 ka interval, and with age uncertainties less than 50% of the event duration. However, we prioritized inclusivity and relaxed this criterion in some instances, such as for the Liuli Cave record (Zhao et al., 2021), to incorporate a broader range of data. Furthermore, we require a method for propagating age uncertainties; we do so with age model ensembles.

## 2.2. Data Sets

Here, we present our speleothem  $\delta^{18}\text{O}$  database (Table 1). We searched the SISAL v3 database (Kaushal et al., 2024) and the literature, from which we extract 14 stalagmite  $\delta^{18}\text{O}$  records from Asia that meet our requirements (Figure 1). For further information on the dynamical context in this region over the mid-Holocene, such as seasonal wind directions, we refer readers to more comprehensive work on the subject (Huo et al., 2021). To remove the effect of insolation (Cheng et al., 2016; Kathayat et al., 2016; Y. Wang et al., 2008) (Figure S2 in Supporting Information S1), all records are detrended using a Savitzky-Golay filter implemented in Pyleoclim (Khider et al., 2022). This allows us to focus on suborbital (centennial-millennial) variability. The detrended  $\delta^{18}\text{O}$



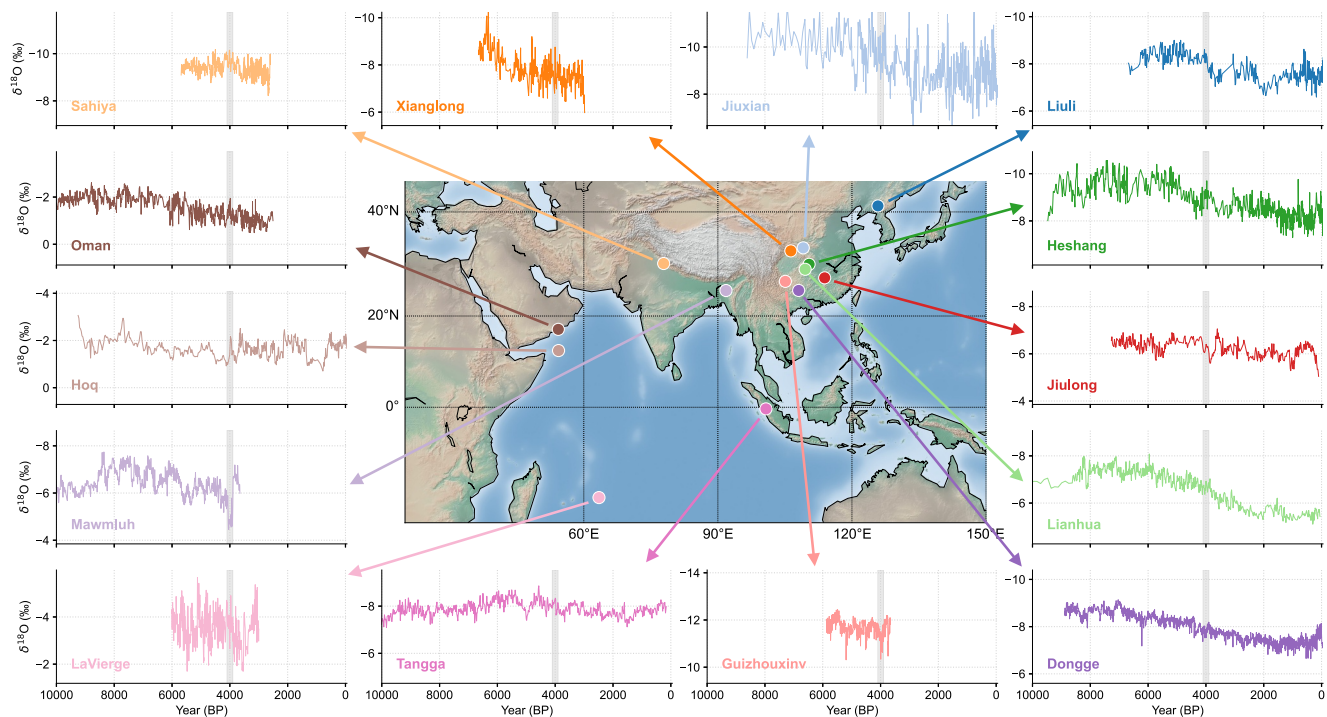


**Figure 1.** Holocene portion of the 14 Asian speleothem  $\delta^{18}\text{O}$  records analyzed in this study, on their published age models. The gray band marks the approximate location of the 4.2 ka BP event.

age ensembles are shown in the left panel of Figure 2. Table 1 contains information on the cave site, stalagmite name, location, time range, resolution, and original publication.

### 2.3. Age Modeling

Age uncertainties must be considered in the investigation of sub-orbital scale variability, particularly when identifying abrupt shifts. Even though the most precise speleothem chronologies can be as accurate as a few years, the age uncertainties of most Holocene Asian speleothem records are in the tens of years. An uncertainty of 50 years can offset two  $\delta^{18}\text{O}$  time series by 100 years, thereby influencing our judgment of how abrupt or synchronous climate conditions were. To account for this, plausible chronologies with 1,000 members each were constructed via the BChron (Parnell et al., 2008) R package, which has been shown suitable for speleothem records (J. Hu et al., 2017; Parnell et al., 2011). Depths, corrected ages, age uncertainties, and measured  $\delta^{18}\text{O}$  of samples from each speleothem records in Table 1 were extracted from the associated publication and converted to the Linked Paleo Data (LiPD) (McKay & Emile-Geay, 2016) format. These variables are the input for the Bchron R package. The age-depth models so constructed are displayed in Figure S1 in Supporting Information S1. This process ensures that all age uncertainty is robustly represented in our results. The way this uncertainty is presented depends on the analytical technique being used. In cases where our analysis produces a time series, we use envelope plots. In the case of the interval statistics technique, we use a mixture of histograms and kernel density estimates. That is, the entirety of the analysis explicitly quantifies age uncertainties, so that all of our results are robust against potential chronological artifacts. In the Supplementary Material, we also supplement many of our analytical pipelines with additional age models independently generated by the COPRA (Breitenbach et al., 2012) and Bacon (Blaauw & Christen, 2011) age model techniques, and show that our results are robust against the choice of age modeling method. In short, age inaccuracies/uncertainty alone cannot explain our results, as we have explicitly and robustly accounted for it at all stages of our analysis.

### 2.4. Synthetic Data

To examine what a well expressed climate event might look like in a collection of speleothem-like series, we created a synthetic version of our data set with an artificial 4.2 ka event. This allows us to manipulate various

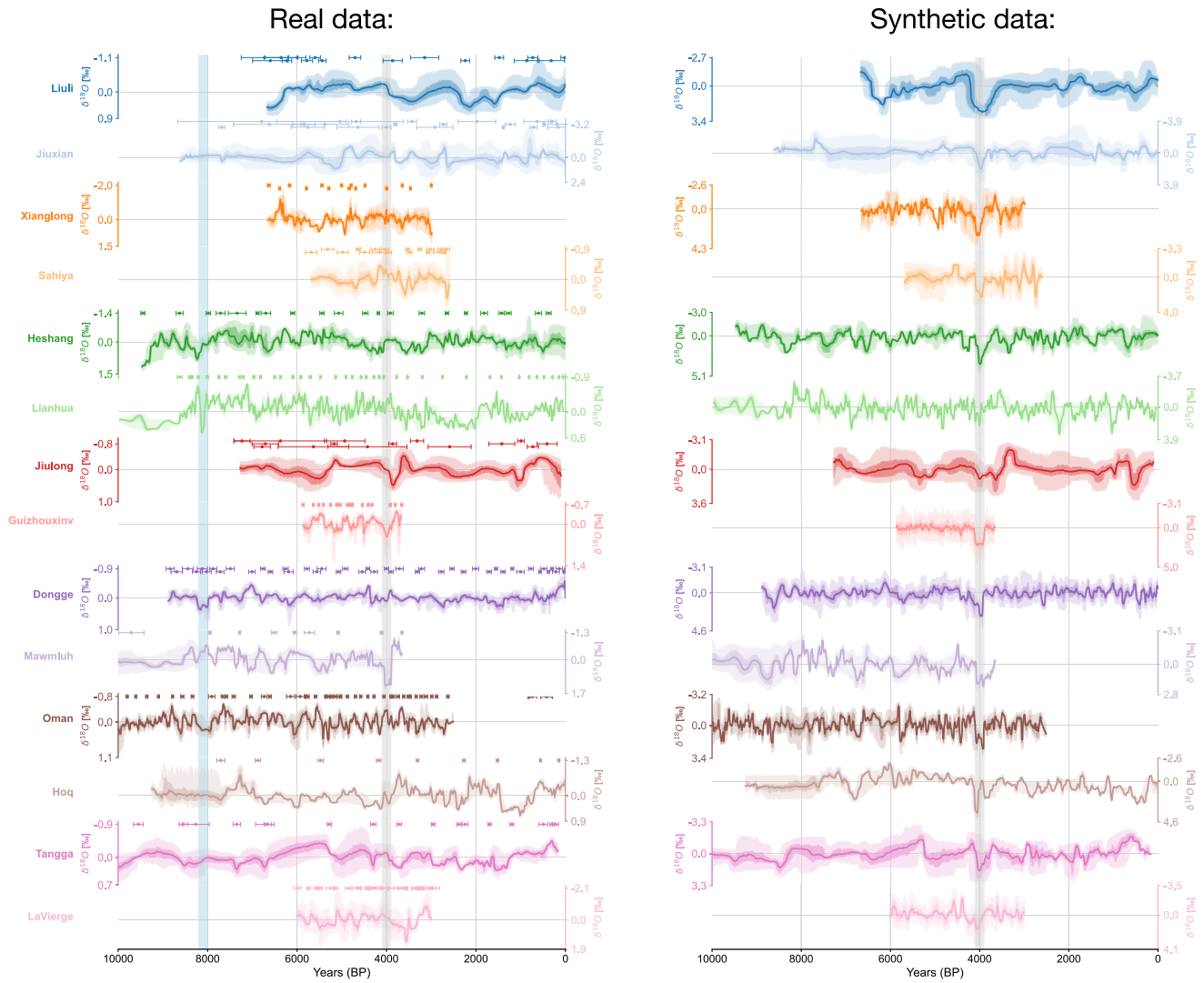


**Figure 2.** Left panel: Detrended  $\delta^{18}\text{O}$  time series from the 14 sites considered in this study (Figure 1, Table 1), with age ensembles. Error bars above each series represent  $^{230}\text{Th}$  ages and  $2\sigma$  intervals. The gray interval denotes 4100–3900 years BP. The blue interval denotes 8200–8000 years BP. Right panel: A synthetic data set with a 4.2 ka event of fixed amplitude and characteristics mimicking the real observations (Section 2.4).

aspects of the analysis protocol in a controlled way, and test the ability of our detection methods (Section 2) to retrieve information about a known event. To create these synthetic records, we generated surrogates of our original time series using an autoregressive process of order 1 (AR(1)). The AR(1) process is a simple stochastic model to simulate processes with short-term memory, where the value at each time point depends on the previous value and a random noise term (Box & Jenkins, 1976), and is conditionally independent of all previous values. For unevenly spaced data, this model can be expressed as follows (Robinson, 1977):

$$X(t_i) = \rho_i X(t_{i-1}) + \varepsilon(t_i), \quad (1)$$

$$\rho_i = \exp\left(-\frac{\Delta t_i}{\tilde{\tau}}\right) \quad (2)$$

where  $X(t_i)$  is the value of the time series at time  $t_i$ ,  $\rho_i$  is the AR(1) coefficient for the time interval  $\Delta t_i = t_i - t_{i-1}$ ,  $\tilde{\tau}$  is the characteristic time scale of the AR(1) process, and  $\varepsilon(t_i)$  is a white noise process with zero mean and constant variance  $\sigma^2$ .

To generate the surrogates, we first estimated the AR(1) persistence parameter,  $\bar{\tau}$ , for the median age ensemble member using the TAUEST algorithm (Mudelsee, 2002) implemented in the Pyleoclim package (Khider et al., 2022). TAUEST uses the method of moments to estimate the persistence of unevenly sampled time series. We then used Equation 1 to generate a surrogate time series with the same temporal resolution as the median ensemble member.

To simulate a 4.2 ka-like event as it appears in the Mawmluh record, we added an asymmetrical spike to each our surrogate time series, with a start time of 4100 years BP and an end time of 3900 years BP. In order to mimic the magnitude of the event in the Mawmluh record, the signal-to-noise ratio (SNR), defined as the amplitude of the spike divided by the standard deviation of the respective ensemble member, was set to 2.0. Other plausible SNR ratios are shown in Figure S4 in Supporting Information S1. We then replaced the real ensemble values with those from the surrogate time series to create surrogate ensembles with realistic age uncertainty. A schematic illustrating this process is shown in Figure S3 in Supporting Information S1, and the resulting stack is shown in Figure 2 (right panel). Further discussion of this stack and its implications can be found in Section 3.1.

## 2.5. Detection Methods

The methods used for evaluating the presence of an event should be chosen such that as many plausible expressions of the event as possible are considered in a statistically robust way. It is well known that purely random, stationary processes can exhibit event-like characteristics (Wunsch, 1999). Changes in variance can appear visually significant even when generated by stationary noise processes (e.g., red noise), which is often a good analog for paleoclimate time series (Meyers, 2012). It is therefore unwise to rely primarily on the eye for a task such as detecting events with paleoclimate data. Appropriate techniques will vary depending on the question/event. In this study, we use interval statistics, LERM, and MC-PCA. These methods are described in more detail below.

### 2.5.1. Interval Statistics

Interval statistics provide a simple, noise-resistant approach that helps to place a particular excursion within the context of the rest of the record. This technique can zero-in on a pre-selected interval, but cannot identify them a priori. The method involves segmenting each timeseries into  $k$  intervals of equal length (corresponding say, to the reported length of an event) and comparing the median value of the target interval (“event”) to those of the other  $k - 1$  intervals. This comparison can be done using traditional histograms or kernel density estimation (KDE), a non-parametric estimate of the underlying probability density function (Emile-Geay, 2023). The analysis can be performed using either the values from the time series itself or the differences between consecutive time steps (in which case it targets the magnitude of transitions). The median value for the target interval is then highlighted or shaded on the histogram or KDE plot of the rest of the median interval values, providing a visual representation of how the event compares to the rest of the record.

### 2.5.2. Laplacian Eigenmaps for Recurrence Matrices

Laplacian Eigenmaps for Recurrence Matrices (LERM) is a non-linear time series analysis technique that tracks changes in the underlying dynamics of the time series. It assumes an underlying coherent dynamical system and benefits from evenly spaced data. The method involves four main steps: (a) phase space reconstruction of the time series via time-delay embedding, (b) generation of a recurrence matrix from the embedded data, (c) calculation of the graph Laplacian and its eigenvectors (eigenmaps) from the recurrence matrix, and (d) computation of a Fisher information statistic from the eigenmaps to track changes in system dynamics over time. Significant changes in the Fisher information statistic are interpreted as indicative of transitions between dynamical regimes. By leveraging the attractor reconstruction capabilities of time-delay embedding (Takens, 1981) and the ability of recurrence plots to capture system dynamics (Webber & Zbilut, 2005), LERM provides a holistic approach to detecting gradual and abrupt transitions in paleoclimate records and other time series data. Further details can be found in James et al. (2024) and Malik (2020).

### 2.5.3. Monte Carlo Principal Component Analysis

Monte Carlo Principal Component Analysis (MC-PCA) is a data reduction technique that helps to distill the main modes of variability present in a set of records, assuming that all the records being evaluated express climate in a similar way. The method is designed to handle time series data with age uncertainties represented by age

ensembles (Anchukaitis & Tierney, 2013; Deininger et al., 2017; Scroxton et al., 2023b). Instead of using a single age model per time series, MC-PCA operates on collections of age ensembles, where each ensemble contains multiple plausible age realizations of a time series. The Monte Carlo aspect involves randomly sampling age realizations from each ensemble and applying standard PCA to this set of sampled time series realizations. This random sampling and PCA calculation is repeated many times using different combinations of age realizations drawn from the ensembles. The resulting distributions of principal components and eigenvalues provide a robust estimate of the dominant modes of variability while fully accounting for age uncertainty in the time series data. By enabling the extraction of common signals from time series data with unavoidable age model errors, MC-PCA proves valuable for paleoclimate reconstructions and other scenarios involving dating uncertainties. The method was implemented using the Pyleoclim package (Khider et al., 2022).

Other methods, such as change point detection techniques (Ruggieri, 2013), were also considered but ultimately excluded. These methods have become increasingly popular in paleoclimatology (McKay et al., 2024; Parker & Harrison, 2022), and are especially useful when handling a large number of records. However, when the database of records can be comfortably plotted in a single stack, such techniques are often unnecessary.

### 3. Results

#### 3.1. The 4.2 ka Event is Minimally Expressed in the Stack

Within our network of speleothem  $\delta^{18}\text{O}$  records there is little evidence of a widespread isotopic enrichment during the 4.2 ka interval. Figure 1 shows the records to exhibit both positive and negative excursions around 4.2 ka, but few of these anomalies emerge as distinctive transitions in the context of the last  $\sim 10,000$  years. In the left panel of Figure 2 we show the detrended age ensembles for each of these records, with associated tie points and tie point uncertainties. Three of the 14 records presented here (Mawmluh, Jiulong, and Guizhouxiny) show visual indication of an enrichment episode around this time. It is also worth noting that records from Shennong (H. Zhang, Zhang, et al., 2021), Anjohibe (L. Wang et al., 2019), and Anjohikely (Scroxton et al., 2023a) experience hiatuses around 4.2 ka. These records were not included in our analysis due to resolution constraints, but do offer support for the existence of a period of strong aridity during the 4.2 ka interval, as low growth rates in speleothems can be interpreted as a moisture signal (Fairchild & McMillan, 2007). The combination of these hiatuses with the appearance of the 4.2 ka event in a minority of the records we examine here suggests the possible presence of a relevant regional climate event. However, were the 4.2 ka an event of global significance (as necessary to define a GSSP), we would expect to observe a robust signal in a much larger proportion of high-resolution continuous speleothems, especially in a network of records located close to the strongest signal of the event.

Another way to approach this detection problem is to probe how a coherent event would manifest in a network of synthetic speleothems with properties that mimic the observed one. One such scenario is presented in the right panel of Figure 2, showing an artificial 200y event centered at 4.2 ka (see Section 2.4 for details). While it is unlikely that any event would express itself as coherently as the 4.2 ka event does in this synthetic version of our data set, this example provides a target for what we might expect to see in, at minimum, a few of these records if the 4.2 ka event was as widespread and severe as has been suggested. In order to better constrain what this event might look like under different SNR scenarios, we constructed several versions of our stack using events with different amplitudes (Figure S4 in Supporting Information S1). An SNR of 2 or 3 appears to be most consistent with the amplitude of the event in the Mawmluh record. In extremely low SNR scenarios (SNR = 0.5), the event is largely undetectable. However, even in the SNR = 1 scenario, in which the maximum expression of the event is notably more subtle than in KM-A, the presence of an isotopic excursion during the event interval is more consistently expressed than in the actual data set. This suggests that, even assuming low SNR conditions in other caves, we would expect the 4.2 ka event to be at least minimally expressed in more records from our data set than is currently observed if it were regionally significant.

#### 3.2. Interval Statistics Over the 4.2 ka Event Interval

A more quantitative approach to assessing this event is to ask whether any record exhibits a 4.2 ka shift as large and sudden as the one documented in the Mawmluh KM-A record. To quantify how extreme Asian speleothem  $\delta^{18}\text{O}$  is around 4.2 ka, we apply interval statistics as described in Section 2.5.1. Figure 3 shows the probability distribution of the detrended  $\delta^{18}\text{O}$  values over 200-year intervals based on 1,000 plausible age models, highlighting  $\delta^{18}\text{O}$  values around 4.2 ka (4.1–3.9 ka, vertical gray bars). In the Mawmluh KM-A record, the  $\delta^{18}\text{O}$  values around 4.2 ka stand

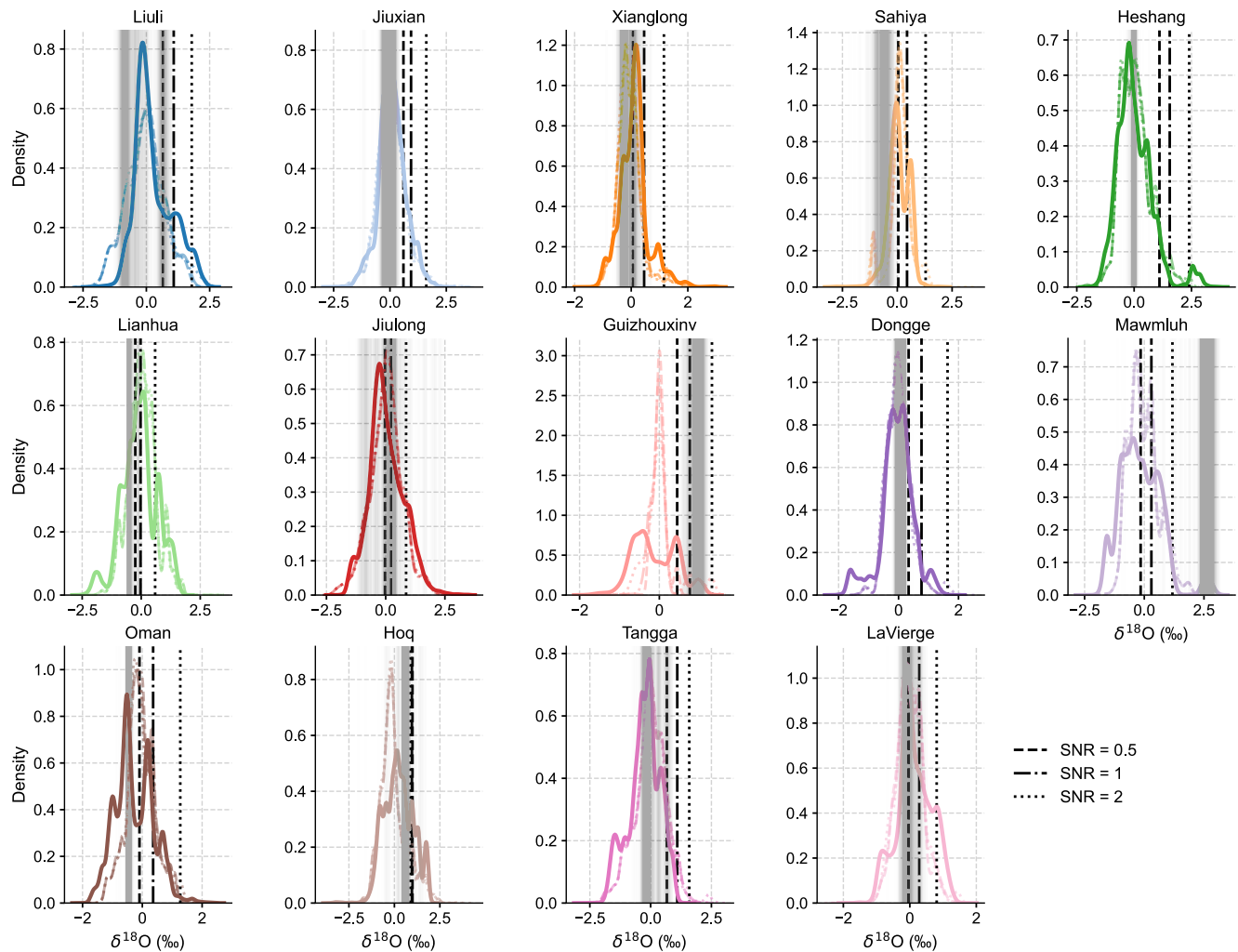


**Figure 3.** The distribution of the detrended  $\delta^{18}\text{O}$  values of the 14 Holocene speleothem records over 200 year intervals based on 1,000 plausible age models generated by BChron. The gray vertical lines are  $\delta^{18}\text{O}$  values in the window surrounding 4.2 ka event interval (4.1–3.9 ka). The solid curves depict the distributions of the real, detrended data. The lower transparent curves depict the distributions of the synthetic versions of the original series with events of different SNRs. Dashed corresponds to an SNR of 0.5, dash-dotted an SNR of 1, and dotted an SNR of 2. The black vertical lines indicate the median  $\delta^{18}\text{O}$  value for the synthetic ensemble during the event interval for each SNR scenario.

out in the context of the Holocene. However, for other Asian speleothem records, the  $\delta^{18}\text{O}$  values for the period centered on the 4.2 ka interval appear typical of average conditions. Guizhouxinv is the only record that shows a significantly positive shift in  $\delta^{18}\text{O}$  values. The  $\delta^{18}\text{O}$  shift at Sahiya and Liuli are both negative during that period, opposite from Mawmluh cave. The synthetic ensembles indicate what the result would look like for events of varying impact. Notably, synthetic ensembles with an event SNR of 0.5 (indicated by the dashed line) record more anomalous  $\delta^{18}\text{O}$  values during the event interval than most of the real ensembles. An SNR of 2 (the dotted line) consistently produces  $\delta^{18}\text{O}$  event interval values that appear anomalous within the context of the KDE. This result is also robust to the age modeling method used (Figures S8 and S9 in Supporting Information S1). It could be argued that a more relevant metric is the rate of change of  $\delta^{18}\text{O}$ , defined as the difference between consecutive intervals. This difference is presented in Figure S10 in Supporting Information S1 for an interval length of 200 years. Mawmluh and Guizhouxinv are again the only records that consistently stand out over the 4.2 ka interval when age uncertainties are considered. Hoq and Tangga may also show some signal during this period, though in the case of Tangga the result is inconsistent when age uncertainty is taken into account. Sensitivity analysis (Figures S13 and S14 in Supporting Information S1) shows that these results are robust to the choice of interval size.



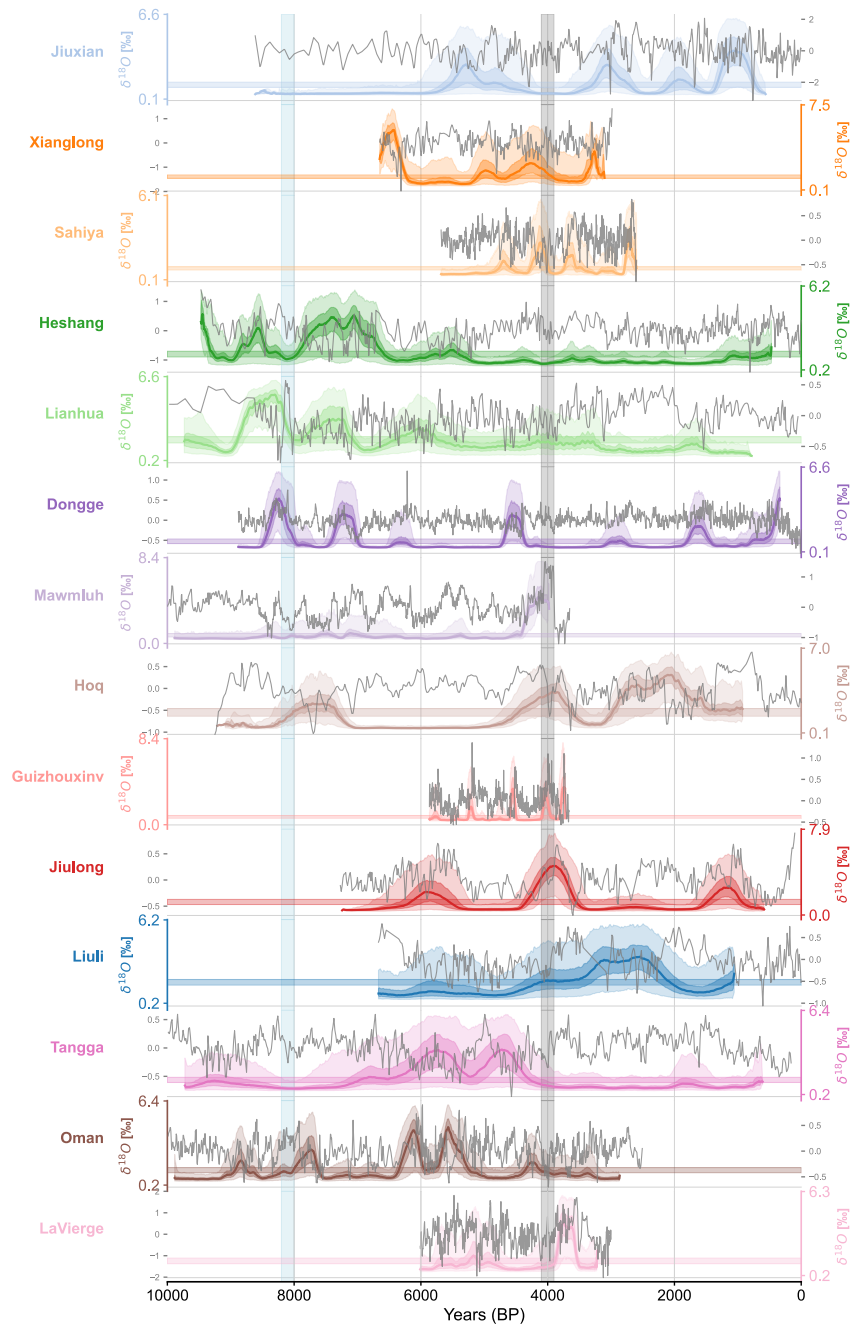


**Figure 4.** Laplacian Eigenmaps for Recurrence Matrices (LERM) applied to our network of speleothem  $\delta^{18}\text{O}$  ensembles. The vertical gray bar indicates the 4.2 ka interval, the vertical blue bar indicates the 8.2 ka event interval. The colored horizontal bars indicate the confidence interval for the Fisher information statistic drawn from the median ensemble member.

### 3.3. Regime Changes With LERM Around the 4.2 ka Interval

The above analyses focused on the magnitude of speleothem  $\delta^{18}\text{O}$  change around the 4.2 ka period; we now look for changes in the dynamical character of these records. Such a change would indicate a regime shift in the climate state governing the formation of these proxies. To carry out this search we apply LERM (Section 2.5.2) to our set of ensembles. This technique is designed to detect when a significant shift has occurred in the dynamics of the system represented by our time series. In this case, that system is the Asian monsoon, represented by some mixture of the amount effect, moisture transport, and moisture source, filtered by cave-specific processes. Figure 4 shows the results of this analysis. There are four parameters that need to be set: embedding dimension

( $m$ ), time delay ( $\tau$ ), window size ( $w_{\text{size}}$ ) and window increment ( $w_{\text{inc}}$ ). Embedding dimension and time delay have the strongest effect on the analysis of paleoclimate records (James et al., 2024). For this work we selected  $m = 10$  and  $\tau$  as equal to the first minimum of mutual information (Abarnabel, 1997).  $w_{\text{size}}$  and  $w_{\text{inc}}$  are arbitrarily taken as 20 and 3 respectively. While changing the configuration of  $m$  and  $\tau$  values shifted the precise timing of detection for certain regime transitions, the results were qualitatively unchanged (Figure S15 in Supporting Information S1). Note that the detection of the beginning of a regime shift often occurs early due to the process of time delay embedding (James et al., 2024). This “smearing” of the detection window is unidirectional, as only information from future time steps is included for a given time embedding. Significant transitions in dynamics are indicated by a crossing of the Fisher information statistic across the plotted confidence interval.

Figure 4 confirms the existence of regime changes near the 4.2 ka event interval in the Jiulong, Guizhouxinv and Mawmluh records. It also suggests that Sahiya, Xianglong, and Hoq may undergo transitions during this period as well. The precise nature of what this change may have been is unclear. Jiulong, Guizhouxinv, and Mawmluh all experience large excursions in  $\delta^{18}\text{O}$  values during this period, which is likely what LERM is detecting. In the case of Sahiya, the dynamical transition is probably related to the negative excursion in its values around this period. In Hoq and Xianglong, the interpretation is less clear, suggesting a more subtle change in dynamics.

Given the presence of dynamical transitions near the 4.2 ka event interval in multiple records, we cannot conclusively rule out a regime shift in climate dynamics during this time period. However, the precise nature of this change remains unclear, as only a few caves record an abrupt change in  $\delta^{18}\text{O}$ , and the timing of the transition is inconsistent. By way of comparison, most of the East Asian records that cover the 8.2 ka interval suggest a significant change in dynamics around this time. Less evidence of a strong response to the 8.2 ka event is observed in the lower latitude regions of our data set (Indonesia and the western edge of the Indian Ocean Basin), which is consistent with more comprehensive work on the topic (Parker & Harrison, 2022).

As we observe a coherent shift in dynamics during the 8.2 ka event despite its epicenter residing in the North Atlantic (Barber et al., 1999), we would expect to observe at least as strong a signal during the 4.2 ka interval near its epicenter if it were globally significant. The relative coherence of an 8.2 ka event signal in our data set compared to that of the shift around 4 ka suggests that the latter was substantially less impactful. This transition may have been related to an isotopic enrichment trend driven by changes in the strength of El Niño–Southern Oscillation (ENSO), a possibility we discuss further in Section 4. However, additional work, such as applying LERM to a broader set of records from SISAL v3, is necessary to better constrain the driver, spatial extent and coherence of this shift.

### 3.4. MC-PCA and Evidence for the Double Drying Hypothesis in East Asia

In order to quantify shared patterns of behavior, we apply Monte Carlo Principal Component Analysis (MC-PCA, (Anchukaitis & Tierney, 2013; Deininger et al., 2017)) to our data set. In order to emulate the workflow of Scroton et al. (2023b), we do not detrend the data before applying this analysis. To avoid noise from other sections of the data set, each record is sliced so that only the time period between 5 ka and 3 ka is being analyzed. We find that both Pattern 1 and Pattern 2 of the Double Drying hypothesis (Scroton et al., 2023b) are robustly represented in 13 of the 14 speleothem records in our data set. We do not observe any significant indication of Pattern 3 (see Figure 2 of Scroton et al. (2023b)) in the dominant modes of variability for these records. Figure 6 shows the spatial loadings of the first principal component. The dominant feature of this component is the strong isotopic enrichment trend from  $\sim 3.9$  ka to 3.6 ka (Pattern 2), positioned on top of a more gradual, long term enrichment trend (Pattern 1). This component is observed coherently with strong positive loadings in all seven speleothem records governed by the East Asian monsoon (Liuli, Jiuxian, Xianglong, Heshang, Lianhua, Jiulong, Guizhouxinv), and four of the five records governed by the Indian monsoon (Sahiya, Oman, Tangga, La Vierge). An additional record from Liang Luar cave (Griffiths et al., 2009), not included in our broader analysis due to resolution constraints, records a hiatus that contains this interval, potentially indicating more arid conditions during this period as far as South East Indonesia. The only record that loads in the opposite direction is from Hoq. The reason for this is unclear, but it is likely a cave-specific, rather than regional, effect. There is some indication of the presence of Pattern 3 in the second principal component, but the spatial footprint is inconsistent and the event itself is not robustly represented (Figure S16 in Supporting Information S1). The variance explained by the second mode is also roughly a third of that explained by the first mode, indicating it as a substantially less significant pattern of shared variance (see Figure 5). This lends further evidence to the interpretation of the 4.2 ka

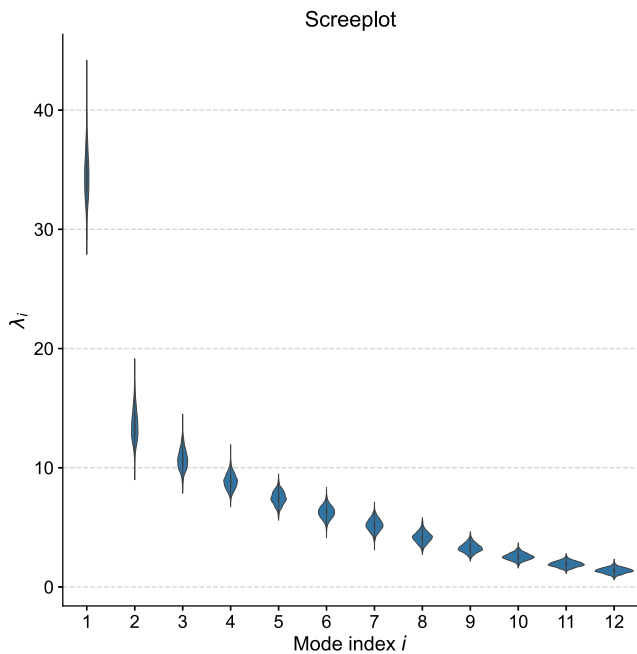


**Figure 5.** The screeplot for MC-PCA applied to our set of speleothem oxygen isotope data.

event as a climate phenomena of potentially regional, rather than global, significance, or one which is not associated with Indian Summer Monsoon change.

We also carry out this analysis on the detrended data, as well as isolated sets containing just the East Asian speleothems and just the Indian Ocean Basin speleothems (see Figures S16–S21 in Supporting Information S1). Despite the application of detrending and the use of regionally isolated speleothem sets, the presence of an enhanced isotopic enrichment trend from 3.9 ka to 3.6 ka and the lack of a clear isotopic excursion in the 4.2 ka event interval remains consistent. This indicates that the findings presented in this study are robust, regardless of the specific speleothems selected or the detrending process employed. Note that Guizhouxin and Mawmluh were excluded from the main analysis due to their short time axes, which would prevent us from examining coherent regional trends after 3.7 kyrs BP. We conducted additional MC-PCA analyses including the Mawmluh and Guizhouxin records in the full group. An isotopic enrichment trend beginning around 3.9 kyrs BP remained the dominant signal present in the first principal component (Figure S22 in Supporting Information S1). We do observe some indication of a brief period of isotopic enrichment from 4.1 to 3.9 kyrs BP in the second principal component of the full set of records (Figure S23 in Supporting Information S1). However, the direction of the loadings was inconsistent across the study region, suggesting that the event had a weak regional impact.

#### 4. Discussion

While there is growing evidence supporting a regionally significant drying event in the Middle East during the 4.2 ka interval (Carolin et al., 2019; Cullen et al., 2000; Sharifi et al., 2015; Watanabe et al., 2019), our analyses do not corroborate previous claims in the literature that this drought was a global occurrence (Walker et al., 2018; Weiss, 2016). We searched for a coherent signal across a region encompassing much of South, Central, and Eastern Asia, an area in the SISAL v3 database with excellent spatial and temporal coverage and the site of

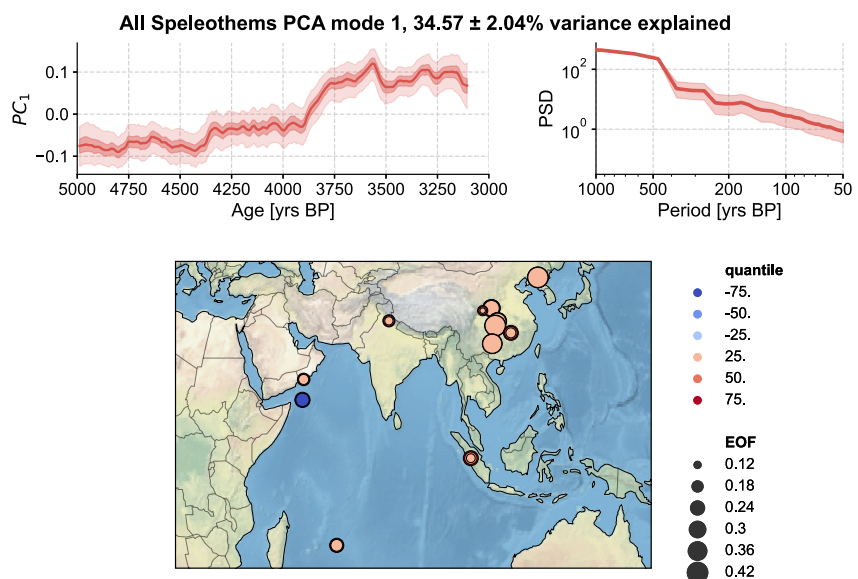


**Figure 6.** MC-PCA applied to all 14 ensembles in our data set, each containing 1,000 members. Marker size indicates EOF value, hue indicates the associated quantile. Cool colors indicate negative loadings while warm colors indicate positive loadings.

Mawmluh Cave, which previously defined the event. We were unable to identify a robust signal that indicated a period of abrupt climate activity during the 4.2 ka interval across Asia. We note that while we combine regions governed by disparate dynamical systems in the ISM and EASM, our analysis primarily examines records individually before synthesizing results, allowing natural separation between regional signals. Additionally, the PCA results remain consistent when analyzing ISM and EASM records separately (Figures S17 and S18 in Supporting Information S1), indicating that combining these regions does not bias our findings. This broad regional analysis is appropriate given claims of the 4.2 ka event's global significance - if the event was globally significant, it should appear in ISM and EASM governed regions, as both are near the proposed center of action.

The simplest explanation for the absence of a coherent 4.2 ka event signal is that the 4.2 ka event was not a global one. Despite its clear expression in the Middle East (Carolin et al., 2019; Theaker et al., 2024), its influence was not widely felt across the Asian monsoon region. Alternatively, the 4.2 ka event was global, but this network of speleothems is ill-equipped to detect the presence of this event. This argument is somewhat circular, as the original record used to define the event, speleothem KM-A from Mawmluh cave (Berkelhammer et al., 2013), is qualitatively similar to all of the records we examine here.

The absence of a coherent 4.2 ka signal within our network of 14 speleothem records is strong evidence for the regional nature of the event. It would be easy to dismiss the evidence from a single record. Indeed, the work of Kathayat et al. (2017, 2018) and Scroxton et al. (2023b) suggests that the KM-A record is not representative of the region as a whole—it is not even representative of other records from the same cave (Figure S5 in Supporting Information S1). It is harder to dismiss 13 other records. Speleothem records are generally considered the most precisely dated of all paleoclimate archives on this timescale (Shen et al., 2013). If they cannot capture this event, very few other records could, with the exception of cross-dated tree-rings, some of which do show an anomaly in 2036 BCE (Salzer et al., 2014). However, speleothems are clearly capable of capturing globally significant climate events that occur over decadal to centennial scales, as attested by the robust presence of the 8.2 ka events in the majority of high-resolution speleothems from around the globe (McKay et al., 2024; Parker & Harrison, 2022). While only about half the records in our data set span the 8.2 ka interval, making its observation tentative, the robust expression of the 8.2 ka event in available records (4 out of 7) contrasts notably with the inconsistent expression of the 4.2 ka event (4 out of 14). This provides further instructive comparison of their relative spatial coherence. A far more likely explanation for the lack of a clearly expressed 4.2ka event in this network is that it was not coherent across Asia, and was therefore not of global significance.

One limitation of this study is the potential for seasonal bias. Speleothems, as hydroclimate recorders, are typically expected to be most sensitive to changes in the behavior of the rainy season. In our study region, this implies sensitivity to changes in the behavior of the Indian Summer Monsoon (ISM) and the East Asian Summer Monsoon (EASM), which drive 90% and 60% of the annual rainfall in the Indian subcontinent (Sahastrabudhe et al., 2023) and East Asia (Sun et al., 2022), respectively. We note that the precise ratio has likely changed over the course of the Holocene (Giesche et al., 2018; Giosan et al., 2018). If the 4.2 ka event primarily expressed itself as a winter drying, as suggested by Scroxton et al. (2023b), speleothems biased toward summer months may not have recorded a significant effect. However, recent work has suggested that speleothems from this region may be sensitive to dry season infiltration (Ronay et al., 2019), indicating that interpreting them solely as recorders of changes in the summer monsoon is likely an oversimplification. Further research is needed to constrain the potential for a winter expression of the 4.2 ka event and to disentangle the seasonal biases of speleothems from these regions.

A feature of Holocene hydroclimate that appears robust across this data set is Pattern 2 of the Double Drying hypothesis (Figure 2 of Scroxton et al. (2023b)). This trend appears in almost all of the speleothem records we examined, and represents a period of changing East Asian monsoon behavior from roughly 3.9 to 3.6 ka. Pattern 2 manifests as a brief intensification of a longer-term, insolation-driven, trend, though its cause is more elusive. Scroxton et al. (2023b) had previously suggested that this pattern was present in paleoclimate proxies from around the Indian Ocean basin. Our work extends this result to the East Asian region, indicating that this trend was expressed in both the Indian and East Asian monsoons. Scroxton et al. (2023b) propose that the presence of Pattern 2 in Indian Ocean Basin records could be linked to more frequent and intense El Niño events, which are known to reduce ISM precipitation (Mooley & Parthasarathy, 1983). This interpretation is supported by recent work showing a notable increase in ENSO variability around 4 ka (Theaker et al., 2024), refining the previous timeline of 5 to 3 ka proposed by Emile-Geay et al. (2016). The East Asian Summer Monsoon's (EASM)

relationship with the ENSO is markedly more complex than that of the ISM (B. Wang et al., 2000). However, recent work has suggested that EASM and ENSO share a predominantly negative relationship on decadal to centennial timescales (Gao et al., 2024; H. Zhang, Cheng, et al., 2018), with stronger El Niño events resulting in periods of weaker EASM, especially during periods of high ENSO variability (Xu et al., 2016). Questions for this interpretation remain, as some studies have suggested that there may be some asymmetry between the response of the EASM to central Pacific versus eastern Pacific ENSO events (D. Jin et al., 2016). We argue that the regime change we observe around 4 ka in our compilation (Section 2.5.2) may reflect changes in the dynamics of the climate system forced by this change in ENSO variability. Further work is necessary to understand the mechanisms behind this regional pattern, as both ENSO-related teleconnections and the interpretation of  $\delta^{18}\text{O}$  signal in speleothems in Asia are imperfectly constrained over the Holocene (J. Hu et al., 2019).

Beyond these events, this analysis has broader implications for the use of speleothem records on suborbital timescales, suggesting that, when the timescale of interest approaches the temporal resolution of the speleothem record and/or the errors in the U-Th ages, then the variability in a single sample should be viewed with extreme caution. In other words, if the coarseness of the record or the errors in the age models are close to the duration of the event, then a single record cannot typify regional or global conditions until it is widely replicated. Over the Holocene, relative age errors on the order of 1% (Dorale et al., 2004) make it difficult to constrain an event that took place over less than several hundred years. However, the widespread presence of a coherent, multi-centennial trend in the form of Pattern 2 drying suggests that speleothems can be consistent recorders of regional hydroclimate signal on longer (multi-centennial to millennial) timescales. The precise nature of what this signal represents from region to region is still debated, and a promising area for future work. For this interpretation to hold at centennial to sub-centennial time scales, it should be quantitatively demonstrated that Asian speleothems display spatially coherent variability at these scales, both through intra- and inter-cave replication. This coherency, or lack thereof, would have profound implications for the way speleothem  $\delta^{18}\text{O}$  records are understood and used over these much shorter timescales of greater relevance to water resource managers.

Given the relatively small amplitude of sub-orbital scale speleothem  $\delta^{18}\text{O}$  variability, establishing the existence of regionally coherent, abrupt events is a frontier problem. Certainly, our community should seek to establish coherency among available records before singling out particular records as representative of the whole. Intra-cave replication is an important safeguard against over-interpretation, as is evidenced by the lack of a robust enrichment event during the 4.2 ka interval in other high resolution stalagmite  $\delta^{18}\text{O}$  data drawn from Mawmluh cave (Figure S5 in Supporting Information S1; see also Scroxton et al. (2023b)). Complementary measurements, such as  $\delta^{13}\text{C}$  and trace elements, could also help exclude non-climate factors and better interpret speleothem  $\delta^{18}\text{O}$  (H. Zhang, Griffiths, et al., 2018). The emergence of community-curated, multiproxy databases like SISAL v3 (Kaushal et al., 2024) is an important step in this direction, as is the broad application of mathematical techniques tailored to detect, and assess the significance of, such events. Until both these tools are in wider use, claims based on a single record should be regarded with great skepticism.

## 5. Conclusion

Through the application of three robust statistical methods, we find little evidence for a coherent, widespread isotopic enrichment during the 4.2 ka interval across our network of Asian speleothem records. Our comprehensive analysis of 14 high-resolution speleothem  $\delta^{18}\text{O}$  records from Asia challenges the notion of a globally significant 4.2 ka event and underscores the spatiotemporal complexity of Holocene hydroclimate variability. Instead, and consistent with the Double Drying hypothesis (Scroxton et al., 2023b), we observe robust support for two patterns: a gradual enrichment trend over the Holocene and a more pronounced enrichment episode from 3.9 to 3.5 ka, consistently expressed across both the Indian Summer Monsoon and East Asian Summer Monsoon regions. These findings cast doubt on the proposal that the 4.2 ka event should mark the onset of a new geologic age, and highlight the need for caution when ascribing global significance to individual paleoclimate records. Our work provides a robust, multi-method, reproducible framework for evaluating the spatio-temporal coherence of paleoclimate events, advancing methodological standards in paleoclimatology. Extending this analysis to a broader set of proxies and regions, investigating the mechanisms behind the observed mid-Holocene climate patterns, and continuing to develop new frameworks for analyzing coherent paleoclimate variability across multiple timescales are all promising lines of future inquiry.



## Data Availability Statement

Code to reproduce all the figures in this work is available at <https://github.com/alexkjames/AsianSpeleothemCoherency/>. Both the data and code necessary for reproduction are fully archived at James (2024).

## Acknowledgments

This work was supported by NSF Grant 2002556. The authors acknowledge the PAGES SISAL working group for assembling a comprehensive collection of quality-controlled speleothem records. We would also like to thank the Center for Advanced Research Computing (CARC) at the University of Southern California for providing computing resources that have contributed to the research results reported within this publication (<https://carc.usc.edu>). We thank the referees for constructive reviews that improved the manuscript.

## References

- Abarnabel, H. D. I. (1997). *Analysis of observed chaotic data*. Springer.
- Adhémar, J. A. (1842). *Révolutions de la Mer: Déluges Périodiques*. Carilian-Goeury et V. Dalmont.
- Anchukaitis, K. J., & Tierney, J. E. (2013). Identifying coherent spatiotemporal modes in time-uncertain proxy paleoclimate records. *Climate Dynamics*, 41(5–6), 1291–1306. <https://doi.org/10.1007/s00382-012-1483-0>
- Arz, H. W., Lamy, F., & Pätzold, J. (2006). A pronounced dry event recorded around 4.2 ka in brine sediments from the northern Red Sea. *Quaternary Research*, 66(3), 432–441. <https://doi.org/10.1016/j.yqres.2006.05.006>
- Barber, D. C., Dyke, A., Hillaire-Marcel, C., Jennings, A. E., Andrews, J. T., Kerwin, M. W., et al. (1999). Forcing of the cold event of 8,200 years ago by catastrophic drainage of Laurentide lakes. *Nature*, 400(6742), 344–348. <https://doi.org/10.1038/22504>
- Bard, E., Antonioli, F., & Silenzi, S. (2002). Sea-level during the penultimate interglacial period based on a submerged stalagmite from Argentarola Cave (Italy). *Earth and Planetary Science Letters*, 196(3–4), 135–146. [https://doi.org/10.1016/s0012-821x\(01\)00600-8](https://doi.org/10.1016/s0012-821x(01)00600-8)
- Battisti, D., Ding, Q., & Roe, G. (2014). Coherent pan-Asian climatic and isotopic response to orbital forcing of tropical insolation. *Journal of Geophysical Research: Atmospheres*, 119(21), 11–997. <https://doi.org/10.1002/2014jd021960>
- Berkehamer, M., Sinha, A., Stott, L., Cheng, H., Pausata, F., & Yoshimura, K. (2013). An abrupt shift in the Indian monsoon 4000 years ago. *Climates, landscapes, and civilizations* (pp. 75–88).
- Blauw, M., & Christen, J. A. (2011). Flexible paleoclimate age-depth models using an autoregressive gamma process. *Bayesian Analysis*, 6(3), 457–474. <https://doi.org/10.1214/11-BA618>
- Box, G., & Jenkins, G. M. (1976). *Time series analysis: Forecasting and control*. Holden-Day.
- Breitenbach, S. F. M., Rehfeld, K., Goswami, B., Baldini, J. U. L., Ridley, H. E., Kennett, D. J., et al. (2012). Constructing Proxy Records from Age models (COPRA). *Climate of the Past*, 8(5), 1765–1779. <https://doi.org/10.5194/cp-8-1765-2012>
- Butzer, K. W. (2012). Collapse, environment, and society. *Proceedings of the National Academy of Sciences*, 109(10), 3632–3639. <https://doi.org/10.1073/pnas.1114845109>
- Cai, Y., Tan, L., Cheng, H., An, Z., Edwards, R. L., Kelly, M. J., et al. (2010). The variation of summer monsoon precipitation in central China since the last deglaciation. *Earth and Planetary Science Letters*, 291(1), 21–31. <https://doi.org/10.1016/j.epsl.2009.12.039>
- Carolin, S. A., Walker, R. T., Day, C. C., Ersek, V., Sloan, R. A., Dee, M. W., et al. (2019). Precise timing of abrupt increase in dust activity in the Middle East coincident with 4.2 ka social change. *Proceedings of the National Academy of Sciences*, 116(1), 67–72. <https://doi.org/10.1073/pnas.1808103115>
- Cheng, H., Edwards, R. L., Shen, C.-C., Polyak, V. J., Asmerom, Y., Woodhead, J., et al. (2013). Improvements in  $^{230}\text{Th}$  dating,  $^{230}\text{Th}$  and  $^{234}\text{U}$  half-life values, and U–Th isotopic measurements by multi-collector inductively coupled plasma mass spectrometry. *Earth and Planetary Science Letters*, 371, 82–91. <https://doi.org/10.1016/j.epsl.2013.04.006>
- Cheng, H., Edwards, R. L., Sinha, A., Spötl, C., Yi, L., Chen, S., et al. (2016). The Asian monsoon over the past 640,000 years and ice age terminations. *Nature*, 534(7609), 640–646. <https://doi.org/10.1038/nature18591>
- Constantin, S., Bojar, A.-V., Lauritzen, S.-E., & Lundberg, J. (2007). Holocene and Late Pleistocene climate in the sub-Mediterranean continental environment: A speleothem record from Poleva Cave (Southern Carpathians, Romania). *Palaeogeography, Palaeoclimatology, Palaeoecology*, 243(3–4), 322–338. <https://doi.org/10.1016/j.palaeo.2006.08.001>
- Cullen, H. M., deMenocal, P. B., Hemming, S., Hemming, G., Brown, F. H., Guilderson, T., & Sirocko, F. (2000). Climate change and the collapse of the Akkadian empire: Evidence from the deep sea. *Geology*, 28(4), 379–382. [https://doi.org/10.1130/0091-7613\(2000\)28<379:ccatco>2.0.co;2](https://doi.org/10.1130/0091-7613(2000)28<379:ccatco>2.0.co;2)
- Dawson, R. R., Burns, S. J., Tiger, B. H., McGee, D., Faina, P., Scroxton, N., et al. (2024). Zonal control on Holocene precipitation in north-western Madagascar based on a stalagmite from Anjohibe. *Scientific Reports*, 14(1), 5496. <https://doi.org/10.1038/s41598-024-55909-6>
- Deininger, M., McDermott, F., Mudelsee, M., Werner, M., Frank, N., & Mangini, A. (2017). Coherency of late Holocene European speleothem  $\delta^{18}\text{O}$  records linked to North Atlantic Ocean circulation. *Climate Dynamics*, 49(1–2), 595–618. <https://doi.org/10.1007/s00382-016-3360-8>
- Dorale, J. A., Edwards, R. L., Alexander, E. C., Shen, C.-C., Richards, D. A., & Cheng, H. (2004). Uranium-series dating of speleothems: Current techniques, limits, & applications. In I. D. Sasowsky & J. Myroie (Eds.), *Studies of cave sediments* (pp. 177–197). Springer US.
- Drysdale, R., Zanchetta, G., Hellstrom, J., Maas, R., Fallick, A., Pickett, M., et al. (2006). Late Holocene drought responsible for the collapse of Old World civilizations is recorded in an Italian cave flowstone. *Geology*, 34(2), 101–104. <https://doi.org/10.1130/g22103.1>
- Emile-Geay, J. (2023). *Data analysis in the Earth & Environmental Sciences* (11th ed.). FigShare. <https://doi.org/10.6084/m9.figshare.1014336>
- Emile-Geay, J., Cobb, K. M., Carre, M., Braconnot, P., Leloup, J., Zhou, Y., et al. (2016). Links between tropical Pacific seasonal, interannual and orbital variability during the Holocene. *Nature Geoscience*, 9(2), 168–173. <https://doi.org/10.1038/ngeo2608>
- Fairchild, I., & McMillan, E. (2007). Speleothems as indicators of wet and dry periods. *International Journal of Speleology*, 36(2), 69–74. <https://doi.org/10.5038/1827-806x.36.2.2>
- Fisher, D., Osterberg, E., Dyke, A., Dahl-Jensen, D., Demuth, M., Zdanowicz, C., et al. (2008). The Mt Logan Holocene–Late Wisconsinan isotope record: Tropical Pacific–Yukon connections. *The Holocene*, 18(5), 667–677. <https://doi.org/10.1177/0959683608092236>
- Gao, K., He, Y., Yang, Y., Jiang, X., Fu, X., Kipkorir, T. M., et al. (2024). Hydroclimate variability over the past 4730 years based on multi-proxy stalagmite records from southwest China. *Palaeogeography, Palaeoclimatology, Palaeoecology*, 642, 112167. <https://doi.org/10.1016/j.palaeo.2024.112167>
- Giesche, A., Staubwasser, M., Petrie, C. A., & Hodell, D. A. (2018). Indian winter and summer monsoon strength over the 4.2 ka BP event in foraminifer isotope records from the Indus River delta in the Arabian Sea. *Climate of the Past*, 15(1), 73–90. <https://doi.org/10.5194/cp-15-73-2019>
- Giosan, L., Orsi, W. D., Coolen, M., Wuchter, C., Dunlea, A. G., Thirumalai, K., et al. (2018). Neoglacial climate anomalies and the Harappan metamorphosis. *Climate of the Past*, 14(11), 1669–1686. <https://doi.org/10.5194/cp-14-1669-2018>
- Griffiths, M. L., Drysdale, R. N., Gagan, M. K., Zhao, J.-X., Ayliffe, L. K., Hellstrom, J. C., et al. (2009). Increasing Australian–Indonesian monsoon rainfall linked to early Holocene sea-level rise. *Nature Geoscience*, 2(9), 636–639. <https://doi.org/10.1038/ngeo605>
- Hu, C., Henderson, G. M., Huang, J., Xie, S., Sun, Y., & Johnson, K. R. (2008). Quantification of Holocene Asian monsoon rainfall from spatially separated cave records. *Earth and Planetary Science Letters*, 266(3), 221–232. <https://doi.org/10.1016/j.epsl.2007.10.015>

- Hu, J., Emile-Geay, J., & Partin, J. (2017). Correlation-based interpretations of paleoclimate data—where statistics meet past climates. *Earth and Planetary Science Letters*, 459, 362–371. <https://doi.org/10.1016/j.epsl.2016.11.048>
- Hu, J., Emile-Geay, J., Tabor, C., Nusbaumer, J., & Partin, J. (2019). Deciphering oxygen isotope records from Chinese speleothems with an isotope-enabled climate model. *Paleoceanography and Paleoclimatology*, 34(12), 2098–2112. <https://doi.org/10.1029/2019pa003741>
- Huo, Y., Peltier, W. R., & Chandan, D. (2021). Mid-Holocene monsoons in South and Southeast Asia: Dynamically downscaled simulations and the influence of the Green Sahara. *Climate of the Past*, 17(4), 1645–1664. <https://doi.org/10.5194/cp-17-1645-2021>
- James, A. (2024). Regimes shifts in Holocene paleohydrology as recorded by Asian speleothems [Software]. *Zenodo*. <https://doi.org/10.5281/zenodo.11094876>
- James, A., Emile-Geay, J., Malik, N., & Khider, D. (2024). Detecting paleoclimate transitions with Laplacian Eigenmaps of Recurrence Matrices (LERM). *Paleoceanography and Paleoclimatology*, 39(1), e2023PA004700. <https://doi.org/10.1029/2023pa004700>
- Jin, D., Hameed, S. N., & Huo, L. (2016). Recent changes in ENSO teleconnection over the western Pacific impacts the eastern China precipitation dipole. *Journal of Climate*, 29(21), 7587–7598. <https://doi.org/10.1175/jcli-d-16-0235.1>
- Jin, G., & Liu, D. (2002). Mid-Holocene climate change in North China, and the effect on cultural development. *Chinese Science Bulletin*, 47(5), 408–413. <https://doi.org/10.1360/02tb9095>
- Jonkers, L., Bothe, O., & Kucera, M. (2021). Preface: Advances in paleoclimate data synthesis and analysis of associated uncertainty: Towards data–model integration to understand the climate. *Climate of the Past*, 17(6), 2577–2581. <https://doi.org/10.5194/cp-17-2577-2021>
- Kathayat, G., Cheng, H., Sinha, A., Berkelhammer, M., Zhang, H., Duan, P., et al. (2018). Evaluating the timing and structure of the 4.2 ka event in the Indian summer monsoon domain from an annually resolved speleothem record from Northeast India. *Climate of the Past*, 14(12), 1869–1879. <https://doi.org/10.5194/cp-14-1869-2018>
- Kathayat, G., Cheng, H., Sinha, A., Spötl, C., Edwards, R. L., Zhang, H., et al. (2016). Indian monsoon variability on millennial-orbital timescales. *Scientific Reports*, 6(1), 24374. <https://doi.org/10.1038/srep24374>
- Kathayat, G., Cheng, H., Sinha, A., Yi, L., Li, X., Zhang, H., et al. (2017). The Indian monsoon variability and civilization changes in the Indian subcontinent. *Science Advances*, 3(12), e1701296. <https://doi.org/10.1126/sciadv.1701296>
- Kaushal, N., Lechleitner, F. A., Wilhelm, M., Azennoud, K., Bühler, J. C., Braun, K., et al. (2024). SISALv3: A global speleothem stable isotope and trace element database. *Earth System Science Data*, 16(4), 1933–1963. <https://doi.org/10.5194/essd-16-1933-2024>
- Khider, D., Emile-Geay, J., Zhu, F., James, A., Landers, J., Ratnakar, V., & Gil, Y. (2022). Pyleoclim: Paleoclimate timeseries analysis and visualization with Python. *Paleoceanography and Paleoclimatology*, 37(10), e2022PA004509. <https://doi.org/10.1029/2022pa004509>
- Lachniet, M. S. (2009). Climatic and environmental controls on speleothem oxygen-isotope values. *Quaternary Science Reviews*, 28(5), 412–432. <https://doi.org/10.1016/j.quascirev.2008.10.021>
- Leipe, C., Demske, D., Tarasov, P. E., & Members, H. P. (2014). A Holocene pollen record from the northwestern Himalayan lake Tso Moriri: Implications for palaeoclimatic and archaeological research. *Quaternary International*, 348, 93–112. <https://doi.org/10.1016/j.quaint.2013.05.005>
- Li, H., Cheng, H., Sinha, A., Kathayat, G., Spötl, C., André, A. A., et al. (2018). Hydro-climatic variability in the southwestern Indian Ocean between 6000 and 3000 years ago. *Climate of the Past*, 14(12), 1881–1891. <https://doi.org/10.5194/cp-14-1881-2018>
- Li, Y., Fleitmann, D., Wang, X., Pérez-Mejías, C., Sha, L., Dong, X., et al. (2023). 550-Year climate periodicity in the Yunnan-Guizhou Plateau during the Late Mid-Holocene: Insights and implications. *Geophysical Research Letters*, 50(11), e2023GL103523. <https://doi.org/10.1029/2023gl103523>
- Li, Y., Wang, N., Zhou, X., Zhang, C., & Wang, Y. (2014). Synchronous or asynchronous Holocene Indian and East Asian summer monsoon evolution: A synthesis on Holocene Asian summer monsoon simulations, records and modern monsoon indices. *Global and Planetary Change*, 116, 30–40. <https://doi.org/10.1016/j.gloplacha.2014.02.005>
- Liu, F., & Feng, Z. (2012). A dramatic climatic transition at ~4000 cal. yr BP and its cultural responses in Chinese cultural domains. *The Holocene*, 22(10), 1181–1197. <https://doi.org/10.1177/0959683612441839>
- Malik, N. (2020). Uncovering transitions in paleoclimate time series and the climate driven demise of an ancient civilization. *Chaos: An Interdisciplinary Journal of Nonlinear Science*, 30(8), 083108. <https://doi.org/10.1063/5.0012059>
- McDermott, F. (2004). Palaeo-climate reconstruction from stable isotope variations in speleothems: A review. *Quaternary Science Reviews*, 23(7–8), 901–918. <https://doi.org/10.1016/j.quascirev.2003.06.021>
- McKay, N. P., & Emile-Geay, J. (2016). The Linked Paleo Data framework—a common tongue for paleoclimatology. *Climate of the Past*, 12(4), 1093–1100. <https://doi.org/10.5194/cp-12-1093-2016>
- McKay, N. P., Kaufman, D. S., Arcusa, S. H., Kolus, H. R., Edge, D. C., Erb, M. P., et al. (2024). The 4.2 ka event is not remarkable in the context of Holocene climate variability. *Nature Communications*, 15(1), 6555. <https://doi.org/10.1038/s41467-024-50886-w>
- Menounos, B., Clague, J. J., Osborn, G., Luckman, B. H., Lakeman, T. R., & Minkus, R. (2008). Western Canadian glaciers advance in concert with climate change circa 4.2 ka. *Geophysical Research Letters*, 35(7), L07501. <https://doi.org/10.1029/2008gl033172>
- Meyers, S. R. (2012). Seeing red in cyclic stratigraphy: Spectral noise estimation for astrochronology. *Paleoceanography*, 27(3), PA3228. <https://doi.org/10.1029/2012PA002307>
- Moerman, J. W., Cobb, K. M., Adkins, J. F., Sodemann, H., Clark, B., & Tuen, A. A. (2013). Diurnal to interannual rainfall  $\delta^{18}\text{O}$  variations in northern Borneo driven by regional hydrology. *Earth and Planetary Science Letters*, 369, 108–119. <https://doi.org/10.1016/j.epsl.2013.03.014>
- Mooley, D. A., & Parthasarathy, B. (1983). Indian summer monsoon and El Niño. *Pure and Applied Geophysics*, 121(2), 339–352. <https://doi.org/10.1007/bf02590143>
- Mudelsee, M. (2002). TAUEST: A computer program for estimating persistence in unevenly spaced weather/climate time series. *Computers & Geosciences*, 28(1), 69–72. [https://doi.org/10.1016/s0098-3004\(01\)00041-3](https://doi.org/10.1016/s0098-3004(01)00041-3)
- Parker, S. E., & Harrison, S. P. (2022). The timing, duration and magnitude of the 8.2 ka event in global speleothem records. *Scientific Reports*, 12(1), 10542. <https://doi.org/10.1038/s41598-022-14684-y>
- Parnell, A. C., Buck, C. E., & Doan, T. K. (2011). A review of statistical chronology models for high-resolution, proxy-based Holocene palaeoenvironmental reconstruction. *Quaternary Science Reviews*, 30(21), 2948–2960. <https://doi.org/10.1016/j.quascirev.2011.07.024>
- Parnell, A. C., Haslett, J., Allen, J. R., Buck, C. E., & Huntley, B. (2008). A flexible approach to assessing synchronicity of past events using Bayesian reconstructions of sedimentation history. *Quaternary Science Reviews*, 27(19), 1872–1885. <https://doi.org/10.1016/j.quascirev.2008.07.009>
- Psomiadis, D., Dotsika, E., Albanakis, K., Ghaleb, B., & Hillaire-Marcel, C. (2018). Speleothem record of climatic changes in the northern Aegean region (Greece) from the Bronze Age to the collapse of the Roman Empire. *Palaeogeography, Palaeoclimatology, Palaeoecology*, 489, 272–283. <https://doi.org/10.1016/j.palaeo.2017.10.021>

- Railsback, L. B., Liang, F., Brook, G., Voarintsoa, N. R. G., Sletten, H. R., Marais, E., et al. (2018). The timing, two-pulsed nature, and variable climatic expression of the 4.2 ka event: A review and new high-resolution stalagmite data from Namibia. *Quaternary Science Reviews*, 186, 78–90. <https://doi.org/10.1016/j.quascirev.2018.02.015>
- Robinson, P. (1977). Estimation of a time series model from unequally spaced data. *Stochastic Processes and their Applications*, 6(1), 9–24. [https://doi.org/10.1016/0304-4149\(77\)90013-8](https://doi.org/10.1016/0304-4149(77)90013-8)
- Roland, T. P., Caseldine, C., Charman, D., Turney, C., & Amesbury, M. (2014). Was there a ‘4.2 ka event’ in Great Britain and Ireland? Evidence from the peatland record. *Quaternary Science Reviews*, 83, 11–27. <https://doi.org/10.1016/j.quascirev.2013.10.024>
- Ronay, E. R., Breitenbach, S. F. M., & Oster, J. L. (2019). Sensitivity of speleothem records in the Indian Summer Monsoon region to dry season infiltration. *Scientific Reports*, 9(1), 5091. <https://doi.org/10.1038/s41598-019-41630-2>
- Ruggieri, E. (2013). A Bayesian approach to detecting change points in climatic records. *International Journal of Climatology*, 33(2), 520–528. <https://doi.org/10.1002/joc.3447>
- Sahastrabudhe, R., Ghausi, S. A., Joseph, J., & Ghosh, S. (2023). Indian summer monsoon rainfall in a changing climate: A review. *Journal of Water and Climate Change*, 14(4), 1061–1088. <https://doi.org/10.2166/wcc.2023.127>
- Salzer, M. W., Bunn, A. G., Graham, N. E., & Hughes, M. K. (2014). Five millennia of paleotemperature from tree-rings in the Great Basin, USA. *Climate Dynamics*, 42(5–6), 1517–1526. <https://doi.org/10.1007/s00382-013-1911-9>
- Scroton, N., Burns, S. J., McGee, D., Godfrey, L. R., Ranivoharimanana, L., Faina, P., & Tiger, B. H. (2023a). Hydroclimate variability in the Madagascar and Southeast African summer monsoons at the Mid- to Late-Holocene transition. *Quaternary Science Reviews*, 300, 107874. <https://doi.org/10.1016/j.quascirev.2022.107874>
- Scroton, N., Burns, S. J., McGee, D., Godfrey, L. R., Ranivoharimanana, L., Faina, P., & Tiger, B. H. (2023b). Tropical Indian Ocean basin hydroclimate at the Mid- to Late-Holocene transition and the double drying hypothesis. *Quaternary Science Reviews*, 300, 107837. <https://doi.org/10.1016/j.quascirev.2022.107837>
- Sharifi, A., Pourmand, A., Canuel, E. A., Ferer-Tyler, E., Peterson, L. C., Aichner, B., et al. (2015). Abrupt climate variability since the last deglaciation based on a high-resolution, multi-proxy peat record from NW Iran: The hand that rocked the Cradle of Civilization? *Quaternary Science Reviews*, 123, 215–230. <https://doi.org/10.1016/j.quascirev.2015.07.006>
- Shen, C.-C., Lin, K., Duan, W., Jiang, X., Partin, J. W., Edwards, R. L., et al. (2013). Testing the annual nature of speleothem banding. *Scientific Reports*, 3(1), 2633. <https://doi.org/10.1038/srep02633>
- Shen, C.-C., Wu, C.-C., Cheng, H., Edwards, R. L., Hsieh, Y.-T., Gallet, S., et al. (2012). High-precision and high-resolution carbonate <sup>230</sup>Th dating by MC-ICP-MS with SEM protocols. *Geochimica et Cosmochimica Acta*, 99, 71–86. <https://doi.org/10.1016/j.gca.2012.09.018>
- Stanley, J.-D., Krom, M. D., Cliff, R. A., & Woodward, J. C. (2003). Short contribution: Nile flow failure at the end of the Old Kingdom, Egypt: Strontium isotopic and petrologic evidence. *Geoarchaeology*, 18(3), 395–402. <https://doi.org/10.1002/gea.10065>
- Staubwasser, M., Sirocko, F., Grootes, P. M., & Segl, M. (2003). Climate change at the 4.2 ka BP termination of the Indus valley civilization and Holocene south Asian monsoon variability. *Geophysical Research Letters*, 30(8), 1425. <https://doi.org/10.1029/2002gl016822>
- Staubwasser, M., & Weiss, H. (2006). Holocene climate and cultural evolution in late prehistoric–early historic West Asia. *Quaternary Research*, 66(3), 372–387. <https://doi.org/10.1016/j.yqres.2006.09.001>
- Sun, M.-A., Sung, H. M., Kim, J., Lee, J.-H., Shim, S., & Byun, Y.-H. (2022). Present-day and future projection of East Asian summer monsoon in Coupled Model Intercomparison Project 6 simulations. *PLoS One*, 17(6), e0269267. <https://doi.org/10.1371/journal.pone.0269267>
- Takens, F. (1981). Detecting strange attractors in turbulence. In D. Rand & L.-S. Young (Eds.), *Dynamical systems and turbulence*, Warwick 1980 (pp. 366–381). Springer Berlin Heidelberg.
- Tan, L., Cai, Y., Cheng, H., Edwards, R. L., Gao, Y., Xu, H., et al. (2018). Centennial-to decadal-scale monsoon precipitation variations in the upper Hanjiang River region, China over the past 6650 years. *Earth and Planetary Science Letters*, 482, 580–590. <https://doi.org/10.1016/j.epsl.2017.11.044>
- Theaker, C. M., Carolin, S. A., Day, C. C., Cobb, K. M., Chen, S., Grothe, P. R., & Couper, H. O. (2024). Borneo stalagmite evidence of significantly reduced El Niño–Southern Oscillation variability at 4.1 kyBP. *Geophysical Research Letters*, 51(6). <https://doi.org/10.1029/2023gl107111>
- Thompson, L. G., Mosley-Thompson, E., Davis, M. E., Henderson, K. A., Brecher, H. H., Zagorodnov, V. S., et al. (2002). Kilimanjaro ice core records: Evidence of Holocene climate change in tropical Africa. *Science*, 298(5593), 589–593. <https://doi.org/10.1126/science.1073198>
- Tian, Y., Fleitmann, D., Zhang, Q., Sha, L., Wassenburg, J. A., Axelsson, J., et al. (2023). Holocene climate change in southern Oman deciphered by speleothem records and climate model simulations. *Nature Communications*, 14(1), 4718. <https://doi.org/10.1038/s41467-023-40454-z>
- Van Rempelbergh, M., Fleitmann, D., Verheyden, S., Cheng, H., Edwards, L., De Geest, P., et al. (2013). Mid-to late Holocene Indian Ocean Monsoon variability recorded in four speleothems from Socotra Island, Yemen. *Quaternary Science Reviews*, 65, 129–142. <https://doi.org/10.1016/j.quascirev.2013.01.016>
- Voosen, P. (2018). New geological age comes under fire. *Science*, 361(6402), 537–538. <https://doi.org/10.1126/science.361.6402.537>
- Walker, M., Head, M. H., Berkehammer, M., Björck, S., Cheng, H., Cwynar, L., et al. (2018). Formal ratification of the subdivision of the Holocene Series/Epoch (Quaternary System/Period): Two new Global Boundary Stratotype Sections and Points (GSSPs) and three new stages/subseries. *Episodes*, 41(4), 213–223. <https://doi.org/10.18814/epiugs/2018/018016>
- Wan, N.-J., Li, H.-C., Liu, Z.-Q., Yang, H.-Y., Yuan, D.-X., & Chen, Y.-H. (2011). Spatial variations of monsoonal rain in eastern China: Instrumental, historic and speleothem records. *Journal of Asian Earth Sciences*, 40(6), 1139–1150. <https://doi.org/10.1016/j.jseas.2010.10.003>
- Wang, B., Wu, R., & Fu, X. (2000). Pacific–East Asian teleconnection: How does ENSO affect East Asian climate? *Journal of Climate*, 13(9), 1517–1536. [https://doi.org/10.1175/1520-0442\(2000\)013<1517:peathd>2.0.co;2](https://doi.org/10.1175/1520-0442(2000)013<1517:peathd>2.0.co;2)
- Wang, L., Brook, G. A., Burney, D. A., Voarintsoa, N. R. G., Liang, F., Cheng, H., & Edwards, R. L. (2019). The African Humid Period, rapid climate change events, the timing of human colonization, and megafaunal extinctions in Madagascar during the Holocene: Evidence from a 2m Anjohibe Cave stalagmite. *Quaternary Science Reviews*, 210, 136–153. <https://doi.org/10.1016/j.quascirev.2019.02.004>
- Wang, P., Clemens, S., Beaufort, L., Braconnot, P., Ganssen, G., Jian, Z., et al. (2005). Evolution and variability of the Asian monsoon system: State of the art and outstanding issues. *Quaternary Science Reviews*, 24(5), 595–629. <https://doi.org/10.1016/j.quascirev.2004.10.002>
- Wang, Y., Cheng, H., Edwards, R. L., An, Z., Wu, J., Shen, C.-C., & Dorale, J. A. (2001). A high-resolution absolute-dated late Pleistocene monsoon record from Hulu Cave, China. *Science*, 294(5550), 2345–2348. <https://doi.org/10.1126/science.1064618>
- Wang, Y., Cheng, H., Edwards, R. L., He, Y., Kong, X., An, Z., et al. (2005). The Holocene Asian monsoon: Links to solar changes and North Atlantic climate. *Science*, 308(5723), 854–857. <https://doi.org/10.1126/science.1106296>
- Wang, Y., Cheng, H., Edwards, R. L., Kong, X., Shao, X., Chen, S., et al. (2008). Millennial- and orbital-scale changes in the East Asian monsoon over the past 224,000 years. *Nature*, 451(7182), 1090–1093. <https://doi.org/10.1038/nature06692>

- Watanabe, T. K., Watanabe, T., Yamazaki, A., & Pfeiffer, M. (2019). Oman corals suggest that a stronger winter shamal season caused the Akkadian Empire (Mesopotamia) collapse. *Geology*, 47(12), 1141–1145. <https://doi.org/10.1130/g46604.1>
- Webber, C., & Zbilut, J. (2005). Recurrence quantification analysis of nonlinear dynamical systems, *Tutorials in Contemporary Nonlinear Methods for the Behavioral Sciences*.
- Weiss, H. (2016). Global megadrought, societal collapse and resilience at 4.2–3.9 ka BP across the Mediterranean and west Asia. *PAGES*, 24(2), 62–63. <https://doi.org/10.22498/pages.24.2.62>
- Weiss, H., Courty, M.-A., Wetterstrom, W., Guichard, F., Senior, L., Meadow, R., & Curnow, A. (1993). The genesis and collapse of third millennium north Mesopotamian civilization. *Science*, 261(5124), 995–1004. <https://doi.org/10.1126/science.261.5124.995>
- Westaway, K. E., Zhao, J.-X., Roberts, R. G., Chivas, A. R., Morwood, M. J., & Sutikna, T. (2007). Initial speleothem results from western Flores and eastern Java, Indonesia: Were climate changes from 47 to 5 ka responsible for the extinction of *Homo floresiensis*? *Journal of Quaternary Science*, 22(5), 429–438. <https://doi.org/10.1002/jqs.1122>
- Williams, B. L., Burns, S. J., Scroxton, N., Godfrey, L. R., Tiger, B. H., Yellen, B., et al. (2023). A speleothem record of hydroclimate variability in northwestern Madagascar during the mid-late Holocene. *The Holocene*, 34(5), 593–603. <https://doi.org/10.1177/09596836231225725>
- Wu, W., & Liu, T. (2004). Possible role of the “Holocene Event 3” on the collapse of Neolithic Cultures around the Central Plain of China. *Quaternary International*, 117(1), 153–166. [https://doi.org/10.1016/s1040-6182\(03\)00125-3](https://doi.org/10.1016/s1040-6182(03)00125-3)
- Wunsch, C. (1999). The interpretation of short climate records, with comments on the North Atlantic and Southern Oscillations. *Bulletin of the American Meteorological Society*, 80(2), 245–255. [https://doi.org/10.1175/1520-0477\(1999\)080<0245:tioscr>2.0.co;2](https://doi.org/10.1175/1520-0477(1999)080<0245:tioscr>2.0.co;2)
- Wurtzel, J. B., Abram, N. J., Lewis, S. C., Bajo, P., Hellstrom, J. C., Troitzsch, U., & Heslop, D. (2018). Tropical Indo-Pacific hydroclimate response to North Atlantic forcing during the last deglaciation as recorded by a speleothem from Sumatra, Indonesia. *Earth and Planetary Science Letters*, 492, 264–278. <https://doi.org/10.1016/j.epsl.2018.04.001>
- Xu, C., Ge, J., Nakatsuka, T., Yi, L., Zheng, H., & Sano, M. (2016). Potential utility of tree ring d18O series for reconstructing precipitation records from the lower reaches of the Yangtze River, southeast China. *Journal of Geophysical Research: Atmospheres*, 121(8), 3954–3968. <https://doi.org/10.1002/2015jd023610>
- Zhang, H., Cheng, H., Sinha, A., Spötl, C., Cai, Y., Liu, B., et al. (2021). Collapse of the Liangzhu and other Neolithic cultures in the lower Yangtze region in response to climate change. *Science Advances*, 7(48), eabi9275. <https://doi.org/10.1126/sciadv.abi9275>
- Zhang, H., Cheng, H., Spötl, C., Cai, Y., Sinha, A., Tan, L., et al. (2018). A 200-year annually laminated stalagmite record of precipitation seasonality in southeastern China and its linkages to ENSO and PDO. *Scientific Reports*, 8(1), 12344. <https://doi.org/10.1038/s41598-018-30112-6>
- Zhang, H., Griffiths, M. L., Chiang, J. C., Kong, W., Wu, S., Atwood, A., et al. (2018). East Asian hydroclimate modulated by the position of the westerlies during Termination I. *Science*, 362(6414), 580–583. <https://doi.org/10.1126/science.aat9393>
- Zhang, H., Zhang, X., Cai, Y., Sinha, A., Spötl, C., Baker, J., et al. (2021). A data-model comparison pinpoints Holocene spatiotemporal pattern of East Asian summer monsoon. *Quaternary Science Reviews*, 261, 106911. <https://doi.org/10.1016/j.quascirev.2021.106911>
- Zhang, H.-L., Yu, K.-F., Zhao, J.-X., Feng, Y.-X., Lin, Y.-S., Zhou, W., & Liu, G.-H. (2013). East Asian Summer Monsoon variations in the past 12.5 ka: High-resolution  $\delta^{18}\text{O}$  record from a precisely dated aragonite stalagmite in central China. *Journal of Asian Earth Sciences*, 73, 162–175. <https://doi.org/10.1016/j.jseaes.2013.04.015>
- Zhao, J., Tan, L., Yang, Y., Pérez-Mejías, C., Brahim, Y. A., Lan, J., et al. (2021). New insights towards an integrated understanding of NE Asian monsoon during mid to late Holocene. *Quaternary Science Reviews*, 254, 106793. <https://doi.org/10.1016/j.quascirev.2020.106793>